01 Jan 1973

# Experimental Measurement of Particle Dispersion in Turbulent Flow

N. M. Howard

C. C. Meek

B. G. Jones

# EXPERIMENTAL MEASUREMENT OF PARTICLE DISPERSION IN TURBULENT FLOW

N. M. Howard, Research Assistant, Nuclear Engineering Program
University of Illinois, Urbana, Illinois
C. C. Meek, Staff Member, Argonne National Laboratory
Argonne, Illinois
B. G. Jones, Professor of Nuclear and Mechanical Engineering
University of Illinois, Urbana, Illinois

## ABSTRACT

The dispersion of particles in turbulent flows, phenomena such as dispersion, diffusion, and sedimentation, and a more fundamental point of view, the description of particle interaction with the turbulent field are recently of increasing interest. A system capable of investigating statistical structure of the motion of particles in a turbulent fluid flow using a turbulent water pipe flow system and particles tagged with CO-60 radioactive pellets has been constructed and tested. The particles were followed in their trajectory by a group of detectors consisting of NaI(Tℓ) crystals mounted on photomultiplier tubes which move with the particles on a movable carriage. From the photomultiplier voltages a time series of particle position and velocity was calculated. Results included Eulerian and convected frame measurements in the underlying fluid field in the pipe, representative measurements from recent experiments with particles, and an analysis of noise and statistical reliability of the results.

## INTRODUCTION

Dispersion of particles in turbulent flows is of increasing interest today. Conservation and pollution research problems are actively concerned with such phenomena as dispersion, diffusion, and sedimentation. From a more fundamental point of view, the description of particle interaction with the turbulent field is of interest. Much work has gone into the development of analytical theories to predict single particle interaction with turbulent flows (1-7). Early experimental investigations with laminar flow (8) and subsequent experiments in turbulent media (9-14) have formed the basis for the present experimental system design. By incorporating optimum experimental conditions and selected design innovations pioneered by others, the detailed statistical structure of the motion of particles in a turbulent fluid flow has been investigated in this system. This enables the validity of analytical theories to be checked.

## EXPERIMENTAL SYSTEM DESIGN CONSTRAINTS

The design of the experimental system has many constraints. For ease of comparison with existing theories of turbulence, the underlying turbulent field should be homogeneous, isotropic and stationary. The particles used must be of sufficiently small size to sample the microscale of the turbulence, and also allow parameterization in size, shape, and density. Since the statistical structure (including the autocorrelation and spectrum) of the particle velocity in the turbulent field is of interest, it is desirable to follow the instantaneous trajectory of the particle as it interacts with the turbulent flow.

Grid-generated turbulence and turbulent pipe flow were considered as the two possible alternatives for providing the turbulent flow field. Grid-generated turbulent flow has low level turbulence intensities and is reasonably homogeneous and isotropic but decays down stream of the grid and a suspended particle would experience a non-stationary field. On the other hand, turbulent pipe flow has the advantage of higher

turbulence intensities and being stationary, but is non-homogeneous and anisotropic in general. However, since the region about the pipe centerline approaches both isotropy and homogeneity, pipe flow was chosen for this study.

The fluid media alternatives for practical reasons were air and water. Although air flow systems are relatively easy to construct, they necessitate the use of very small light particles due to the particle's high relative density. Water flow systems allow more flexibility in the parameterization of particles, but pose some added construction constraints.

Previous experiments by Snyder (9) and by Kennedy (10) used stationary cameras and photographic techniques to observe the particle's trajectory. This technique leads to a discrete time series of a few points along the particle trajectory and to rather cumbersome data processing techniques. Jones, et al. (15) used light emitting particles and photomultiplier detectors to continuously monitor the particle's trajectory. Problems were experienced with low signal-to-noise due to inherently low level intensity sources and with non-steady light emission from the particles.

The experimental design selected for this study uses the modified turbulent water pipe flow system of Jones. However, the particles are tagged with radioactive CO-60 pellets, rather than visible light emitting material, and are followed in their trajectory by a group of detectors consisting of NaI(Tℓ) crystals mounted on photomultiplier tubes.

The advantages of this system are: it allows for continuous analog tracking of the particles; the underlying turbulent flow is relatively homogeneous and isotropic in the core region of the pipe with adequate turbulence intensity; constraints on particle size, density and shape are easier to meet in water; and analysis of the data is simpler than with photographic methods. Early modifications to Jones' system are reported by Jones, et al. (16) and preliminary data taken with this system is reported by Meek (17).

## DESCRIPTION OF THE SYSTEM

A general schematic of the system is shown in Figure 1. The turbulent environment for the particle is maintained by a closed loop system. An Ingersoll-Rand 3VK-15 pump (11.5 horsepower, 400 gpm @ 90 foot head) supplies water to an elevated, isolated header tank with a Borda mouth entrance to the vertical 30-foot long, 7- 1/4-inch ID flow section. The Borda mouth is equipped with screens, radial vanes and a rake assembly to artificially trip the flow, thereby providing nearly fully developed and stationary turbulence in the 17-foot long test section, Figure 1. To assure symmetry of the flow at the 90° elbow exit of the test section, a honeycomb resistance network is inserted in the elbow just below the test section exit. The flow rate of the system is controlled by the loop control valve and is monitored by a U-tube manometer and orifice plate arrangement. To help maintain a constant Reynolds number, the temperature of the water can be regulated by passing hot or cold water through the tubular heat exchanger in the main storage tank. Temperature can be held constant to within $\pm$ 1°F. Pipe Reynolds numbers up to 100,000 are easily attainable.

Insertion, capture and retrieval of the radioactive particle are accomplished by a separate particle injection system, Figure 2. Once the particle has been initially inserted it can be recycled through the system to ensemble measurements. The operation of the valves controlling circulation of the particle is done remotely to reduce radiation exposure to the experimenter. The main particle transport path is 5/8-inch ID clear Tygon tubing through which the particle is pushed by city main water pressure.

The particle tracking system consists of 8 photomultiplier tubes mounted on a movable aluminum carriage as shown in Figure 3. The detectors are operated at a bias voltage of 870 volts. Normal output voltages from the detectors range from 0 to approximately 2.0 volts depending on particle position. The carriage is driven by a Vickers hydraulic pump and drive motor, Figure 4. The weight of the carriage and detectors is counterbalanced so that only system inertia and friction must be overcome by the hydraulic drive. A feedback monitor, coupled to the drive motor, operating off the ZEH and ZEL (axial direction) detector voltage difference, enables the carriage to closely follow the mean axial particle motion. Speed and feedback sensitivity of the carriage drive are controlled variables, selected by the experimenter for the specific particle and fluid flow condition.

The movable carriage feedback tracking system allows for Lagrangian frame measurements to be taken on the particle trajectory.

The particles (Figure 5) used in experimental work are made in various shapes, sizes and densities. The major ingredients used are Pelaspan (an expandable polystyrene plastic), ballast (in the form of small

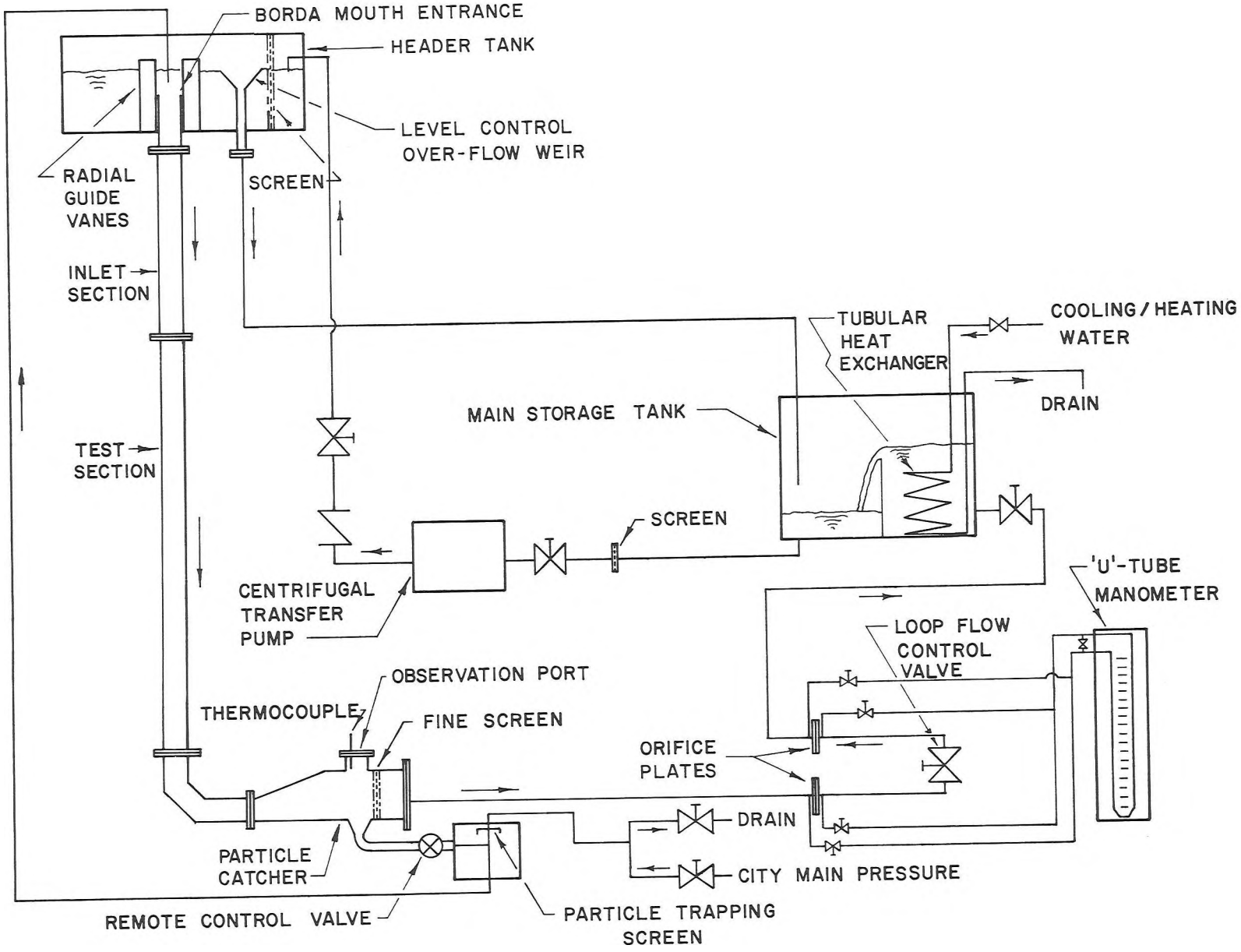


Figure 1. Schematic of particle turbulence loop.

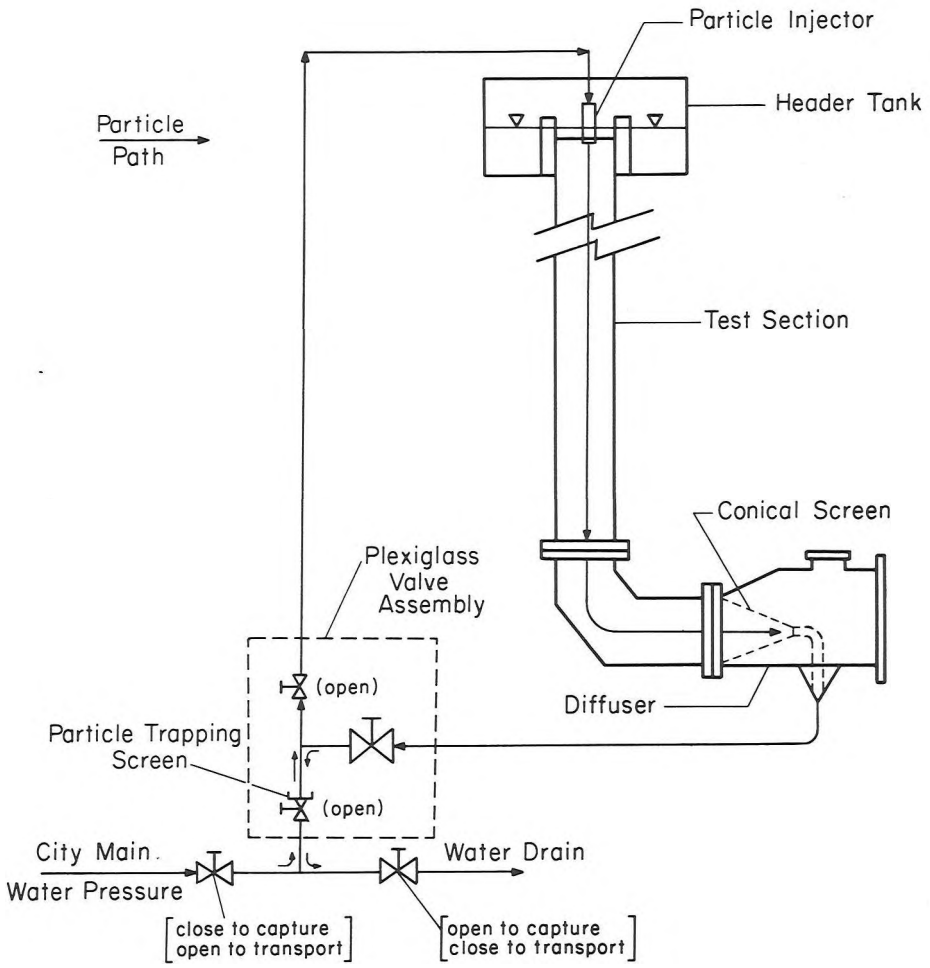


Figure 2. Particle insertion, circulation and removal system.

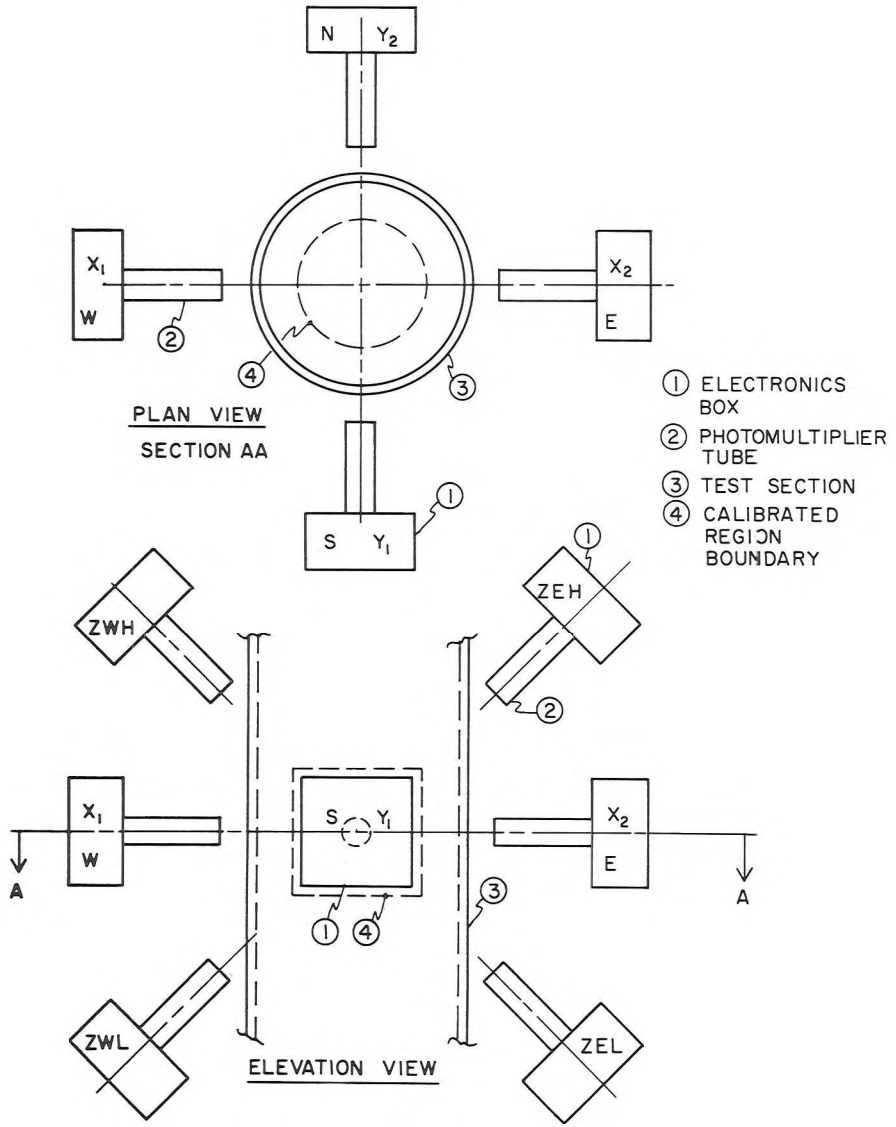


Figure 3. Detector pair physical arrangment.

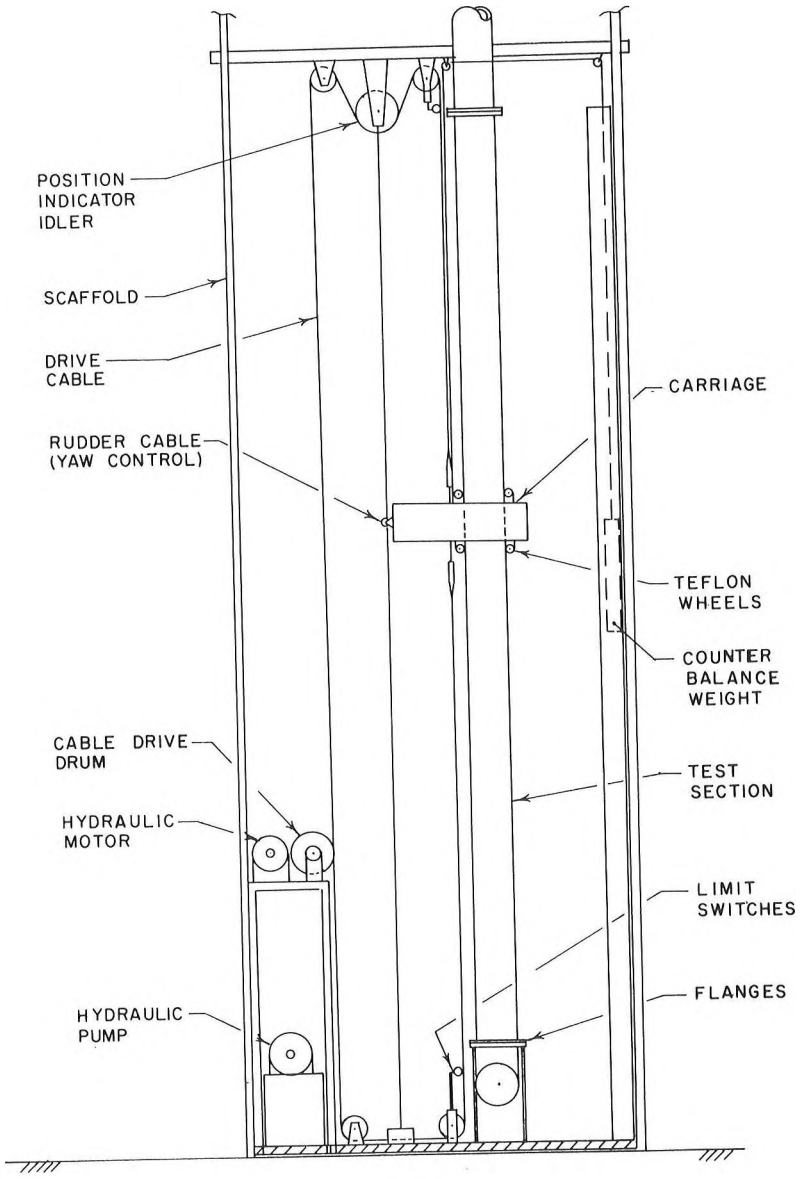


Figure 4. Schematic of carriage support and drive system.

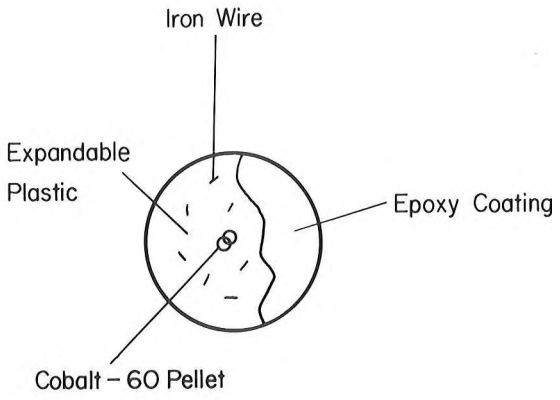


Figure 5. Schematic of fabricated particle.

beads of solder or lead), and a radioactive Co-60 chip of about 10 millicuries strength. The ingredients are placed in an aluminum mold and then immersed in boiling water to allow the plastic to expand and fill the mold. A coat of bright spray lacquer and a coat of clear spray lacquer give the particle better visibility and ruggedness. Particles were made with diameters ranging from 2 mm to 6.5 mm in the shape of spheres and equal volume cubes and tetrahedrons. Density can be regulated to give particle Reynolds numbers based on the quiescent free fall velocity in the range $-200 \leq Re_Q \leq 1000$. (Negative $Re_Q$ refers to a negatively buoyant particle.)

Normal operation of the system during an experiment proceeds as follows: The particle is circulated to the top of the flow section and enters the pipe at the centerline. As the particle is swept through the upper length of the flow section the tape recorder is started. As the particle nears the carriage, waiting at the top of the test section, its approach position is monitored by the axial position sensors and observed on an oscilloscope. The carriage drive and feedback is energized as the particle reaches the center of the calibrated region of the carriage. The data switch is turned on and the tape recorder records the signals transmitted by the carriage as it follows the particle down the test section. Just before the carriage and particle get to the bottom of the test section, the data switch and the tape recorder are turned off. The carriage automatically is stopped by a limit switch and is driven back to the top of the test section while the particle is captured and recycled back to the inlet to the flow section to begin another run. Signals during the run are constantly monitored to assure that the particle remains within the calibrated region during the run.

Work is now underway to modify the present system to accomodate multiparticle loadings of various sizes and densities.

## DATA ACQUISITION AND ANALYSIS

The processes of data acquisition and analysis are shown schematically in Figure 6. The raw voltage signals from the photomultiplier tube detectors are first passed through Bay Laboratories differential amplifiers where the following signals are formed from the eight input signals and the differential signals are filtered at 100 Hz:

$$\Delta X = X1 - X2$$
$$\Delta Y = Y1 - Y2$$
$$\Delta ZE = ZEH - ZEL$$
$$\Delta ZW = ZWH - ZWL$$

The four differential signals are passed through a passive RC filter (30 Hz cutoff) and then recorded at 15 ips on magnetic tape with a Sangamo Model 3560 FM tape recorder. Two signals, POT1 and POT2, from two continuous rotation potentiometers connected to the position indicator idler (Figure 4) and a trigger signal from a 1.5 VDC battery are recorded simultaneously with the detector signals. The potentiometer signals are used in determining the time varying carriage position and velocity. The trigger signal is used as a control signal during subsequent data digitization.

The recorded analog signals are then A/D converted with a Spiras 65 system at a maximum rate of one point per millisecond of real time. For ease in analysis on the computer, the digital tapes from the A/D converter are compressed and formatted with a tape conversion program, TCP, before analysis.

The main analysis program takes the six digital input voltage signals and calculates a time series of the particle's position. Only particle trajectories within the calibrated core region of the pipe are analyzed (see Figure 3). This core region is defined as being the geometric region within the radius of 6 cm about the centerline of the test section which has an inside radius of 9.2 cm. (A discussion of the validity of this region is given later.) The core region is calibrated on a separate apparatus by placing the particle in known positions and recording the voltage signals generated. Data for many different static particle positions are recorded and these voltage-position points are fitted to a three-dimensional third-order polynomial by a least square formula, whose coefficients are generated from calibration data. From these coefficients any given set of voltages from the eight detectors can be converted to a unique particle position in cylindrical coordinates ($r$, $\theta$, $z$).

The particle's velocity time series is calculated by a least squares fit of a straight line to a small increment of the particle position time series. (This is a further averaging process and acts as a digital filter on the data.) The particle velocity autocorrelations are calculated by the lagged product method from the particle's velocity time series in the three

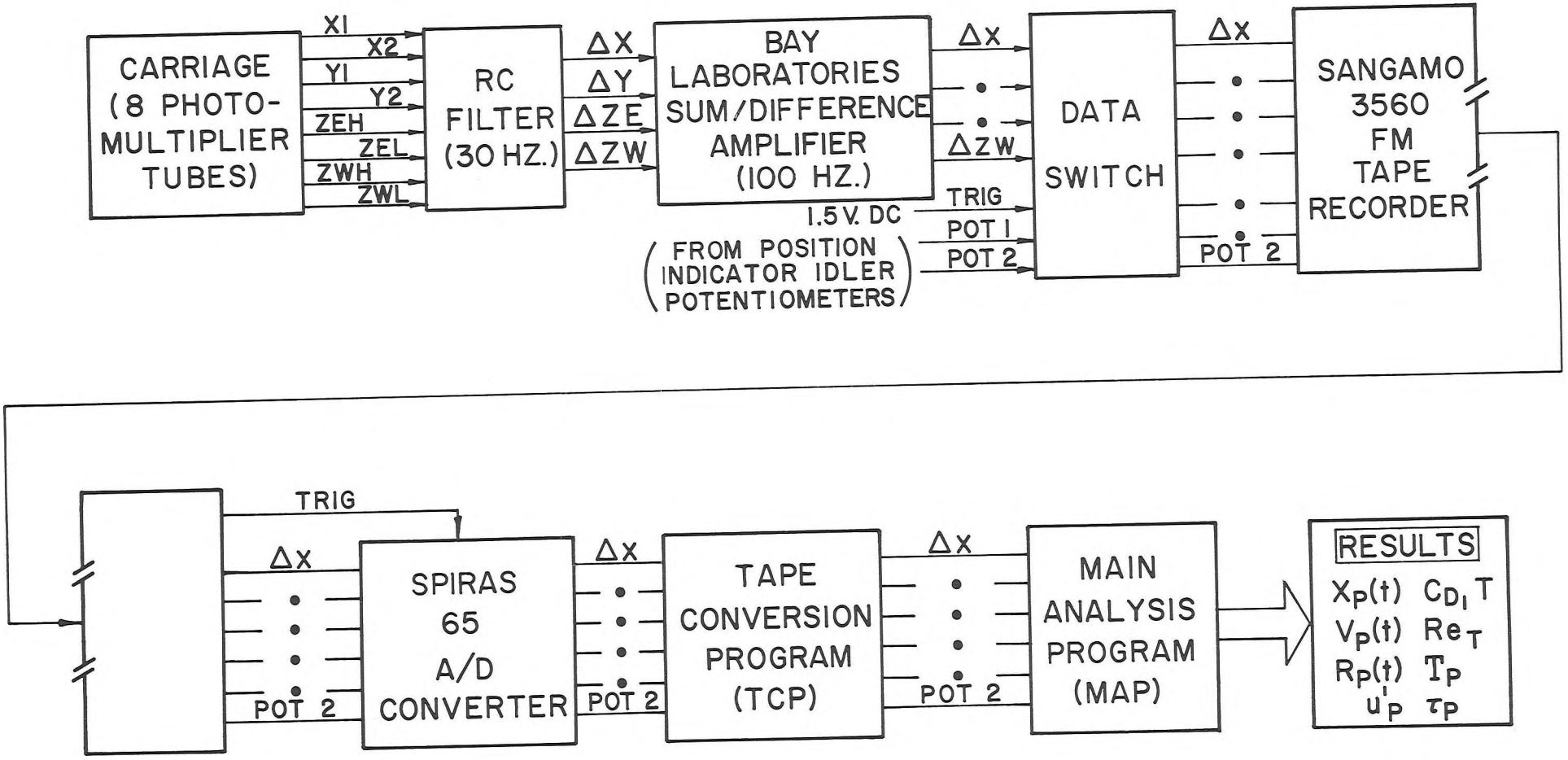


Figure 6. Particle trajectory data acquisition and analysis system.

coordinate directions. Fast Fourier transforms are currently being investigated as an alternate approach, but due to the moderate number of points in the time series is not expected to provide substantial reduction in computational time.

## RESULTS

In order to understand suspended particle motion, knowledge of the underlying fluid field is necessary. Meek (17) made fluid measurements of the mean velocity profile and turbulent intensity profile as shown in Figures 7 and 8. These measurements were also used as inputs to the main analysis program for use in the particle data reduction. The discrepancy in the axial intensity is attributed to the inability of reaching a fully developed turbulent structure for the fluid field in the short development length of this apparatus. However, the fact that little change in this radial dependence occurred over the length of the test section allows the use of an axially constant turbulent structure of measured level. The inclusion of Burchill's (20) data shows the corresponding radial and azimuthal intensity components in fully developed turbulent pipe flow.

From the calibrated core radius of 6 cm ($r/R_o$ = 0.65) the observed variation in mean velocity is small (<15% drop below centerline value). The variation in axial velocity intensity is somewhat larger, but the radial and azimuthal velocity intensities vary significantly less than the axial component in the calibrated region. In addition, the convected frame integral time scale is relatively constant in this region, being 1.5 seconds at the centerline and increasing to about 1.9 seconds at $r/R_o$ = 0.65. Other integral parameters show similar radial variation. Although these radial variations of the turbulent fluid field are somewhat larger than ideal, incorporation of this non-homogeneity into the data processing using experimentally determined radial behavior has been done by Howard (21). It is further argued, since residence of a particle outside the calibrated region during any part of its trajectory during an experimental run removed that run, that the probability of a particle residing near the outside radius of the calibrated region for a significant part of a run was small. Thus, the effective average radius for the particle trajectory is substantially reduced below $r/R_o$ = 0.65 with a correspondingly more uniform fluid turbulence field.

A series of particle runs with the same particle is ensemble averaged to obtain ensembled forms of the particle velocity autocorrelation, Figure 9, and the corresponding velocity power spectrum, Figure 10.

Other quantities of interest calculated from the particle velocity time series include the flatness and skewness as well as the mean and rms particle velocities. The turbulent particle Reynolds number, $Re_T$, and the turbulent particle drag coefficient, $C_{D,T}$, are calculated from the mean axial turbulent free fall velocity, <VZ>, as follows:

for spherical particles

$$Re_T = \frac{\langle VZ \rangle D}{\nu}$$

$$C_{D,T} = \frac{\frac{8}{3} R(\rho_p - \rho_f)g}{\rho_f \langle VZ \rangle^2}$$

for non-spherical particles

$$Re_T = \frac{\langle VZ \rangle VOL_p}{\nu A_p}$$

$$C_{D,T} = \frac{2\, VOL_p\, (\rho_p - \rho_f)g}{A_p\, \rho_f \langle VZ \rangle^2}$$

where <VZ> is determined as the average relative axial velocity between the experimentally observed particle trajectory velocity and the local mean fluid velocity for each run and ensembled for the series of runs for each particle.

Particle macroscales are typically calculated from an integration of the autocorrelation function over the full time range. However, when significant negative lobes occur in the functional, as for the radial and azimuthal particle velocity autocorrelations, underestimates would result in evaluating these time macroscales. As a result both these lateral macroscales were computed by integrating the particle autocorrelation functions to their first zero crossing. Such a limitation was not required for the axial macroscale which was evaluated from

$$T_{p,z} = \int_0^{\tau_{max}} R_{p,z}(\tau)\, d\tau$$

The lateral macroscales were evaluated from

$$T_{p,r} = \int_0^{\tau_{cross}} R_{p,r}(\tau)\, d\tau.$$

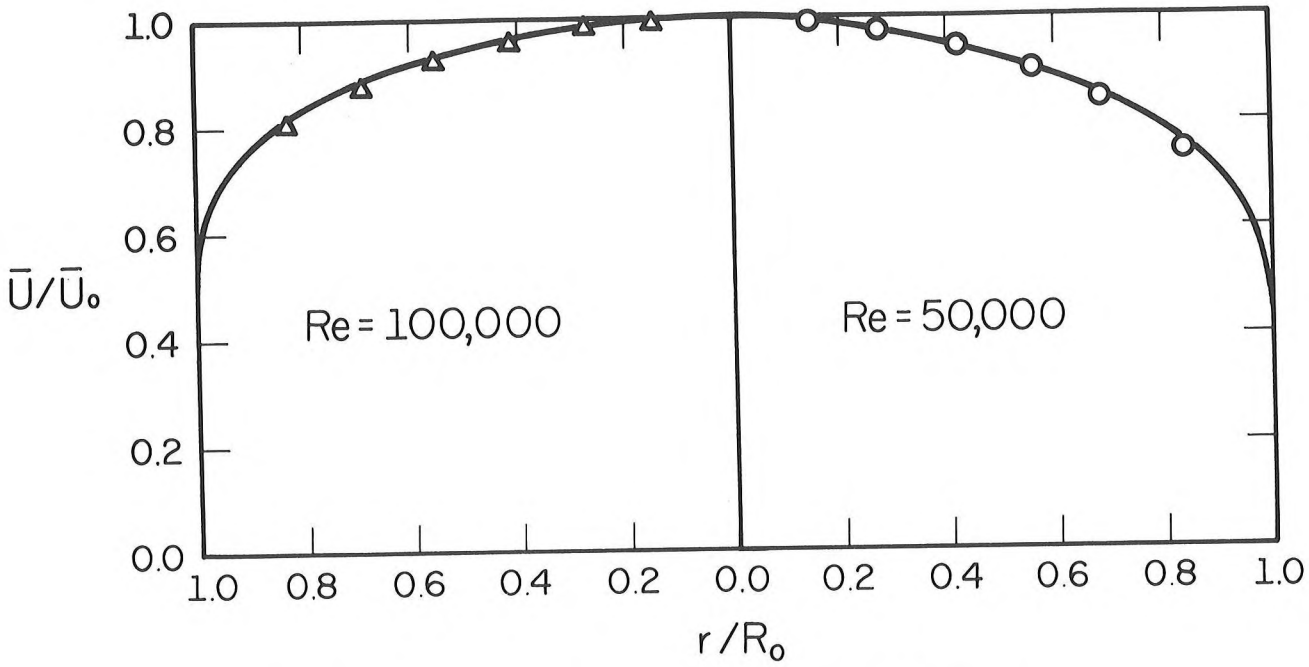


Figure 7. Mean axial fluid velocity profiles.

Re = 100,000
Δ Present experiment
— Nikuradse's (18) data

Re = 50,000
0 Present experiment
— Laufer's (19) data

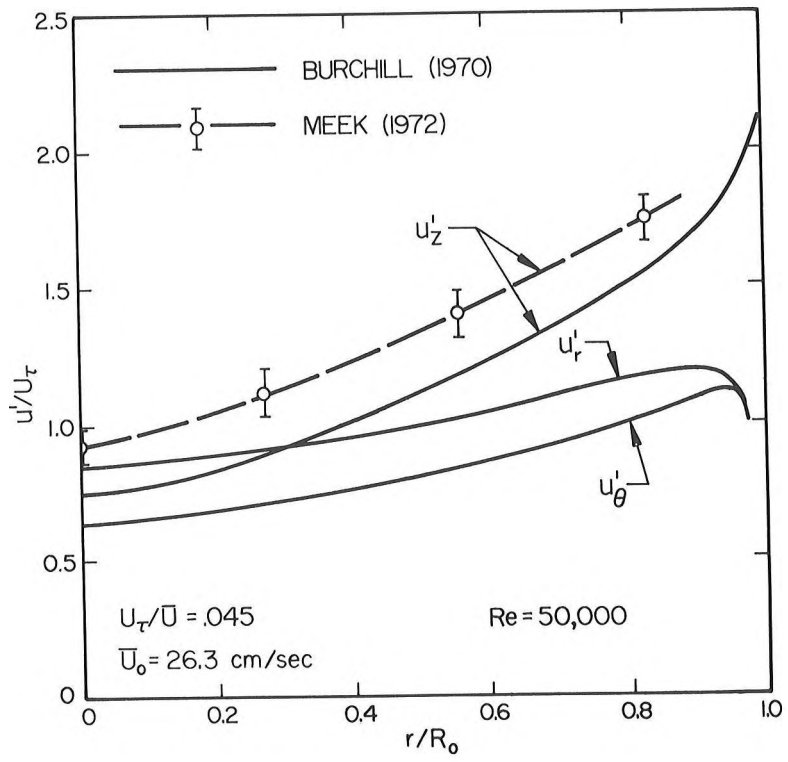


Figure 8. Radial variation of axial velocity turbulence intensity in the fluid.

—— present experiment
--- Burchill's (20) data

In these integrations $R_{p,i}(\tau)$ were determined for the $i^{th}$-coordinate direction from an evaluation for each experimental run on the instantaneous fluctuating velocity of the particle through the relation

$$R_{p,i}(\tau) = \frac{\langle u_{p,i}(t)\, u_{p,i}(t+\tau)\rangle}{(\langle u_{p,i}^2(t)\rangle)^{1/2}(\langle u_{p,i}^2(t+\tau)\rangle)^{1/2}}$$

and the results ensembled for the particle series. The time averages ($\langle\ \rangle$) are performed over the length of each run of about 10 seconds, depending on the free fall particle velocity. Figure 9 shows these three autocorrelations.

The microscales were determined from a parabolic functional fit to the $R_{p,i}(\tau)$ over the initial curvature. This method was selected over the integration of the spectrum since the high frequency spectrum behavior for these ensembled results was not sufficiently rapidly decreasing to give negligible contribution. The autocorrelations were fit by

$$R_{p,i}(\tau) \cong 1 + k_{m,i}\,\tau^2$$

over an initial length $\tau$ defined so that the least squares error in the fit parameter, $k_{m,i}$, was less than 1%. The associated microscale, $\tau_{p,i}$, is given by

$$\tau_{p,i} = \sqrt{-1/k_{m,i}}$$

These scales and other associated turbulent particle velocity structure parameters are tabulated in Table 1 for the 39 runs of the FFP1 series for a 6.5 mm diameter spherical particle with $Re_Q$ = 135. The corresponding autocorrelations and related spectra are presented in Figures 9 and 10. Each spectrum was determined from a least squares fit of a Guassian-cosine series to the ensembled autocorrelation. The cosine transform was then applied using the $R_{p,i}(\tau)$. The normalization of the resulting spectrum was set so that the area under each spectrum was unity.

All of the results shown in this section have been corrected for statistical uncertainty due to the radioactive emission of the particle labeling source. The following section examines these errors and discusses their relative magnitudes.

Table 1. Statistical Properties of the Particle Motion for $Re_Q$ = 135 in FFP1 Series

| | | |
|---|---|---|
| rms Fluctuating Particle Velocity | $V'_{p,r}$ | 0.83 cm/sec |
| | $V'_{p,\theta}$ | 0.91 cm/sec |
| | $V'_{p,z}$ | 2.05 cm/sec |
| Flatness* | $F_{p,r}$ | 3.04 |
| | $F_{p,\theta}$ | 3.47 |
| | $F_{p,z}$ | 2.89 |
| Skewness* | $S_{p,r}$ | -0.32 |
| | $S_{p,\theta}$ | 0.33 |
| | $S_{p,z}$ | -0.08 |
| Macroscale | $T_{p,r}$ | 0.28 sec |
| | $T_{p,\theta}$ | 0.38 sec |
| | $T_{p,z}$ | 0.76 sec |
| Microscale | $\tau_{p,r}$ | 0.46 sec |
| | $\tau_{p,\theta}$ | 0.49 sec |
| | $\tau_{p,z}$ | 0.40 sec |
| Turbulent Reynolds Number | $Re_T$ | 221 |
| Turbulent Drag Coefficient | $C_{D,T}$ | 0.34 |

*These values are for particle velocities without correction for radioactive decay noise.

SOURCES OF ERROR

To estimate the accuracy of the experimental system a series of controlled error particle experiments was performed. With the carriage in a stationary position, a test particle was inserted at different axial positions inside the calibrated region. Signals from this configuration were processed in the same manner as an actual dynamic particle run. Comparison of the position and velocity values calculated by the analysis

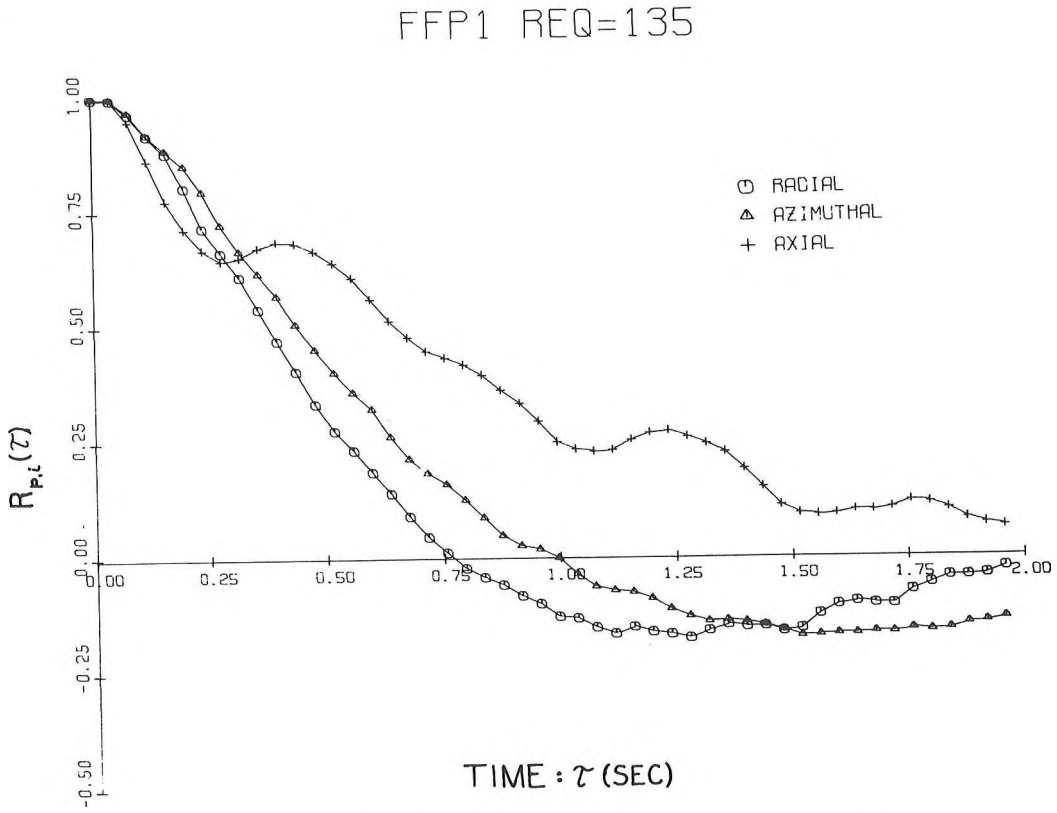


Figure 9. Ensembled autocorrelations for particle fluctuating velocities in radial, azimuthal and axial directions.

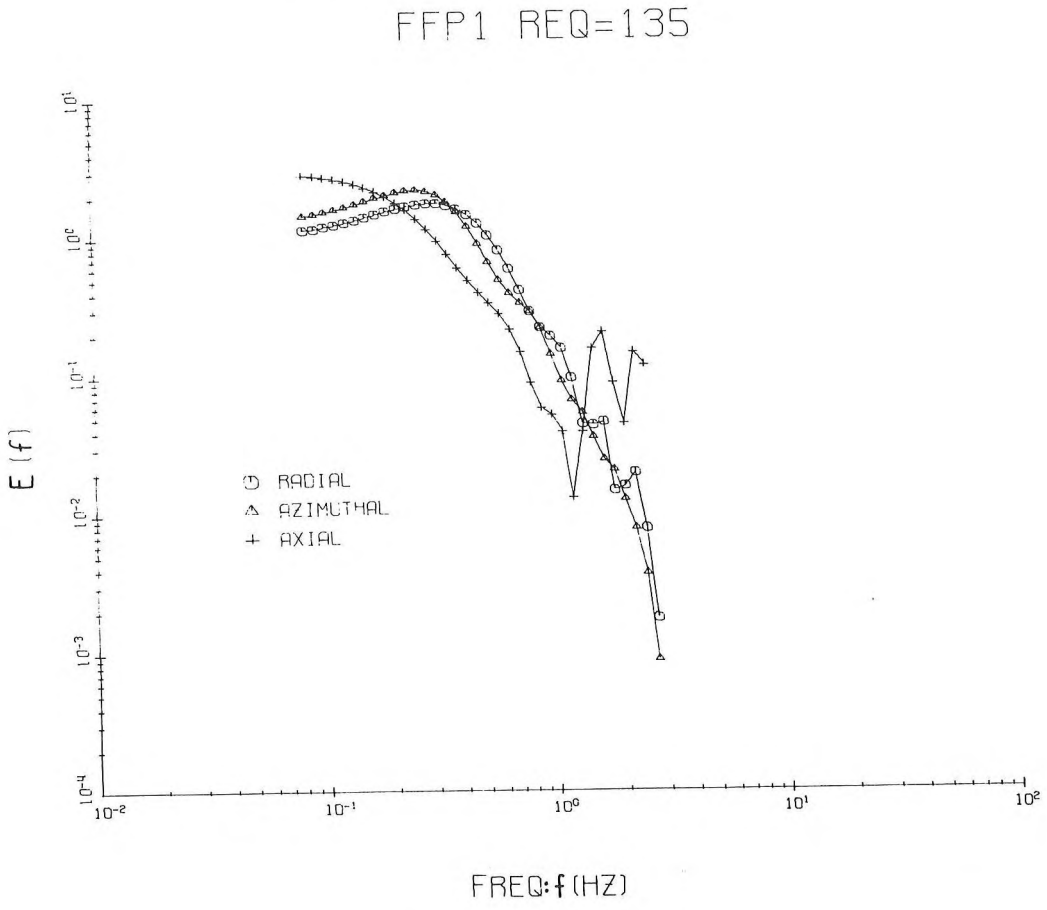


Figure 10. Ensembled power spectral densities for particle fluctuating velocities in radial, azimuthal and axial directions.

scheme with the known actual values of position and velocity yield the cumulative error inherent in the acquisition and analysis procedures.

The results of these error experiments show the rms variations of the absolute positions, the instantaneous relative positions and the instantaneous velocities in Table 2. The observed variation of these uncertainties is found to be relatively insensitive to particle location in the calibrated core region.

To apply corrections to $R_{p,i}(\tau)$, it is observed that the uncertainty from particle random emission is not statistically coupled to the turbulent particle motion. Thus, a simple method of algebraically subtracting the error from the original particle determination is employed and is included in Figures 9 and 10. This results in a statistical error of up to 20% in the particle macroscales in typically ensembled results of 20 to 30 runs in the ensemble.

One of the direct ways of improving the accuracy of the ensemble is to increase the number of runs in the ensemble. This is readily seen to improve the accuracy proportional to $1/\sqrt{M}$, where M is the number of runs in the ensemble.

## APPLICATIONS OF THE RESULTS TO DISPERSION

In parallel with the experimental program described in this study, an analytical program to develop suitable engineering models for predicting suspended particle behavior in known turbulent fluid fields was conducted. The experimental data provides a means for determining the suitability of the prediction models. Details of the analytical program are beyond the scope of this discussion and are reported by Meek (17) and Howard (21). To provide an example of the utility of the data and the success of the analytical predictions Figure 11 provides a comparison of the theory with the experiment for the axial dispersion of the FFP1 particle in the pipe flow of this study. The agreement is particularly good, showing the utility of this experimental study and in addition the appropriateness of the model.

## SUMMARY AND CONCLUSIONS

A description of an experimental system for monitoring detailed trajectories of particles suspended in a well documented turbulent flow field has been presented. Some of the unique features, including the continuous monitoring of three-diemnsional trajectories and the data processing procedures, have been presented in detail. It was shown that the system also allows a wide parameterization of the particle-fluid interactions. A set of typical experimental results was included to demonstrate the utility of the system. Statistical uncertainty errors have been discussed and their experimental values were presented. From these results it is concluded that the facility possesses significant potential and capacity to study the statistical structural details of particle dispersion in turbulent flow.

## ACKNOWLEDGMENTS

This project was sponsored under grant USDI 14-31-0001-3582 from the Department of the Interior and by the University of Illinois at Urbana-Champaign. This support is gratefully acknowledged.

## SYMBOLS

| | |
|---|---|
| $A_p$ | maximum cross sectional area of particle |
| $C_{D,T}$ | particle turbulent drag coefficient |
| D | particle diameter (for spherical particles) |
| E(f) | normalized particle energy spectrum |
| $F_{p,i}$ | flatness of particle velocity time series for $i^{th}$ direction |
| f | particle free fall velocity in quiescent fluid; cyclical frequency |
| g | acceleration of gravity |
| $k_m$ | microscale fit parameter |
| R | particle radius |
| $Re_Q$ | particle quiescent Reynolds number = $\frac{fD}{\nu}$ |
| $Re_T$ | particle turbulent Reynolds number = $\frac{<VZ>D}{\nu}$ |
| $R_{p,i}(\tau)$ | particle velocity autocorrelation for $i^{th}$ direction |
| $S_{p,i}$ | skewness of particle velocity time series for $i^{th}$ direction |
| U | total fluid velocity |
| u | fluctuating fluid velocity |
| $VOL_p$ | volume of the particle |
| $V'_{p,i}$ | rms particle velocity for $i^{th}$ direction |
| <VZ> | particle axial free fall velocity in turbulent fluid |
| $\nu$ | kinematic viscosity of the fluid |

Table 2. RMS Statistical Uncertainties in Evaluated Particle Behavior

| Quantity | Radial | Azimuthal | Axial |
|---|---|---|---|
| Absolute Position | 0.26 cm | 0.08 rad | 0.08 cm |
| Instantaneous Relative Position | 0.026 cm | 0.010 rad | 0.055 cm |
| Instantaneous Particle Velocity | 0.63 cm/sec | 0.54 cm/sec | 1.17 cm/sec |

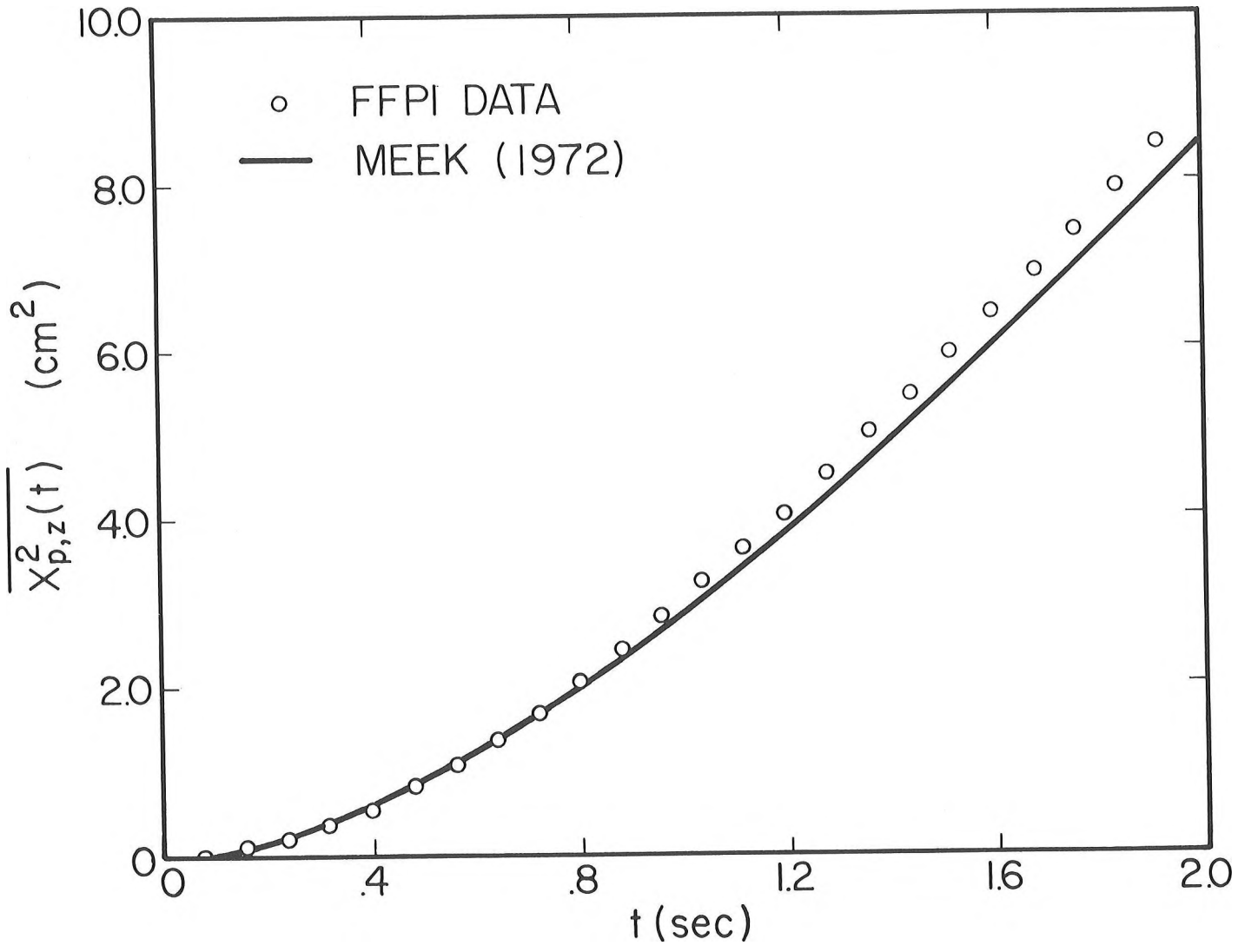


Figure 11. Comparison of experimental axial dispersion data and analytical predictions.

| | |
|---|---|
| $\rho_f$ | fluid density |
| $\rho_p$ | particle density |
| $\tau_{p,i}$ | particle time microscale for $i^{th}$ direction |
| $T_{p,i}$ | particle time macroscale for $i^{th}$ direction |

Subscripts

| | |
|---|---|
| f | relates to fluid |
| i | relates to i-th direction (r,θ,z) |
| p | relates to particle |
| Q | relates to quiescent fluid condition |
| T | relates to turbulent |
| τ | relates to shear |

Superscripts

| | |
|---|---|
| ' | denotes rms of fluctuating component |
| - | temporal average |

REFERENCES


1. Lumley, J. L., "Some Problems Connected with the Motion of Small Particles in Turbulent Fluid," Ph.D. Thesis, The Johns Hopkins University (1957).

2. Chao, B. T., "Turbulent Transport Behavior of Small Particles in Dilute Suspension," Osterreichisches Ingenieur-Archiv, 18, 7 (1964).

3. Hinze, J. O., Turbulence, McGraw-Hill Book Co., Inc., New York, p. 352 (1959).

4. Peskin, R. L., "Stochastic Estimation Applications to Turbulent Diffusion," Stochastic Hydraulics, Proceedings of the International Symposium on Stochastic Hydraulics, Pittsburgh, University of Pittsburgh Press, p. 251 (1971).

5. Brodkey, R. S., The Phenomena of Fluid Motions, Addison-Wesley Publishing Co., Reading, Mass., p. 621 (1967).

6. Friedlander, S. K., "Behavior of Suspended Particles in a Turbulent Fluid," AIChE J., 3, 381 (1957).

7. Meek, C. C., and Jones, B. G., "Studies of the Behavior of Heavy Particles in a Turbulent Fluid Flow," J. Atmos. Sci., 30, 239 (1973).

8. Segré, G., and Silverberg, A., "Behavior of Macroscopic Rigid Spheres in Poiseuille Flow, Part 1 - Determination of Local Concentration by Statistical Analysis of Particle Passages through Crossed Light Beams," J. Fluid Mech., 14, 115 (1962).

9. Snyder, W. H., and Lumley, J. L., "Some Measurements of Particle Velocity Autocorrelation Functions in a Turbulent Flow," J. Fluid Mech., 48, 41 (1971).

10. Kennedy, D. A., "Some Measurements of the Dispersion of Spheres in a Turbulent Flow," Ph.D. Thesis, The Johns Hopkins University (1965).

11. Vanoni, V. A., and Brooks, W. H., "A Study of Turbulence and Diffusion Using Tracers in a Water Tunnel," Hydrodynamic Laboratory, California Institute of Technology Report E-46 (1955).

12. Ginsberg, T., "Droplet Transport in Turbulent Pipe Flow," ANL Report 7694 (1971).

13. Murray, S. P., "Settling Velocities and Vertical Diffusion of Particles in Turbulent Water," J. Geophysical Res., 75, 1647 (1970).

14. Jones, B. G., et al., "Transport Processes of Particles in Dilute Suspension in Turbulent Water Flow - Phase II," University of Illinois Water Resources Center Research Report No. 58 (1972).

15. Jones, B. G., et al., "An Experimental Study of Small Particles in a Turbulent Fluid Field Using Digital Techniques for Statistical Data Processing," Dev. in Mech., 4, 1249 (1968).

16. Jones, B. G., et al., "Transport Processes of Particles in Dilute Suspension in Turbulent Water Flow - Phase I," University of Illinois Water Resources Center Research Report No. 40 (1971).

17. Meek, C. C., "Statistical Characterization of Dilute Particulate Suspensions in Turbulent Fluid Fields," Ph.D. Thesis, University of Illinois at Urbana-Champaign (1972).

18. Nikuradse, J., "Strömungsgetze in Rauhen Rohren," Forschungshaft, 361 (1933).

19. Laufer, J., "The Structure of Turbulence in Fully Developed Pipe Flow," NACA Report 1174 (1954).

20. Burchill, W. E., "Statistical Properties of Velocity and Temperature in Isothermal and Nonisothermal Turbulent Pipe Flow," Ph.D. Thesis, University of Illinois at Urbana-Champaign (1970).

21. Howard, N. M., "Experimental Measurements of Particle Motion in a Turbulent Pipe Flow," Ph.D. Thesis, University of Illinois at Urbana-Champaign (1974).

DISCUSSION

W. G. Tiederman, Oklahoma State: Would you define the Reynolds number of the particle again?

Jones: The quiescent Reynolds number of the particle is based on its free fall velocity in quiescent fluid (f), its hydraulic diameter (D) and the kinematic viscosity of the fluid ($\nu$) (in this case water) and given by the relation $fD/\nu$.

Tiederman: Since you used the density difference between the particle and the water there is not any ambiguity about density, but what diameter do you use when the particle is something other than a sphere?

Jones: In the non-spherical case we have chosen an alternate definition for the hydraulic diameter. In an attempt to relate to the drag coefficient and to the inertial aspects of the particle, we define the hydraulic diameter as the ratio of the particle volume to its maximum cross sectional area. However, there would appear to be no universal convention so that an explicit definition must accompany the quoted values.

Tiederman: Do you have plans to try and relate the fluctuation of the turbulence?

Jones: The theories for which we are trying to provide verification data do predict the turbulent velocity fluctuations of the particle with respect to the velocity structure of the fluid turbulence.

C. A. Sleicher, University of Washington: From your data can you calculate a kind of Lagrangian integral scale?

Jones: Yes, we can calculate, from particle data, the particle's Lagrangian integral scale, but not that of the fluid.

Sleicher: That was my question, whether or not you had compared it to the fluid integral scale.

Jones: The agreement will depend on how well the particle follows the turbulence. We have not made the comparison since we have not made the fluid measurements. We are planning to make two point space-time correlations with hot-film anemometry to estimate the fluid Lagrangian integral time scale for comparison with what we calculate based on particle measurements.

R. H. J. Sellin, University of Bristol: Do you intend to explore particle interaction effects and could you do this by having a single marked particle falling in a cloud of unmarked particles? I would have thought particle interaction effects very important in any sediment or particle movement study.

Jones: This is true and, as I mentioned, this is the extension that we are now planning for our studies. We plan to incorporate a single tagged particle in a multi-particle loading of particles with the same size and the same density characteristics so that we can determine the effects of such interactions in comparison to the single particle motion in dilute suspension.

I would like to make a comment concerning some of the questions which have centered around results that we are reluctant to present at this point. We have varied the density of the tagged particle from near neutral bouyancy, which we would then anticipate should follow relatively closely the fluid turbulence, provided the particle diameters are smaller than the fludi turbulence structure. We have made measurements with lighter than and heavier than fluid particles, but the relative densities of the particle and fluid are not significantly different. With present particle size limitations of greater than 3mm diameter, making particles with densities significantly different than the fluid cause the free fall particle Reynolds numbers to be too large. So we are limited somewhat in the range of the relative density parameters. But we can certainly examine the particle free fall velocity effect on its turbulent response. We can examine also the effect of shape on the response, but we are somewhat restricted at the moment in examining the inertia effects, which become much more important when the particle is heavy as compared to the suspending fluid. For most of the people here, in the laser-Doppler work, the inertia effects are critical for air systems. However, in the water systems I think we can make some reasonably good studies that relate to such laser-Doppler applications. Although we cannot shrink the particle quite small enough to retain Stokes' drag behavior, we can certainly examine the inertia effect and compare this with what can be kept in the analytical analyses if linearization of the viscous drag is accepted.